Universität Karlsruhe (TH)
Institut für Baustatik

A 3D-Plasticity Model for the Description of Concrete and its 3D-FE-Implementation

J. Schütt, W. Wagner

Mitteilung 2(2003)

BAUSTATIK

Universität Karlsruhe (TH)
Institut für Baustatik

A 3D-Plasticity Model for the Description of Concrete and its 3D-FE-Implementation

J. Schütt, W. Wagner

Mitteilung 2(2003)

BAUSTATIK

© Prof. Dr.–Ing. W. Wagner
Institut für Baustatik
Universität Karlsruhe
Postfach 6980
76128 Karlsruhe

Telefon: (0721) 608–2280
Telefax: (0721) 608–6015
E–mail: bs@.uni-karlsruhe.de
Internet: http://www.bs.uni-karlsruhe.de

A 3D-Plasticity Model for the Description of Concrete and its 3D-FE-Implementation

J. Schütt, W. Wagner

Institut für Baustatik, Universität Karlsruhe,

Kaiserstr. 12, D-76131 Karlsruhe, Germany

Abstract

A three-dimensional material law is introduced which is based on a multi-surface plasticity theory for small strains. Different yield criteria of the Drucker-Prager type in combination with a spherical segment to include all-side-compression are used. The special formulation of the yield-function leads only to a small number of necessary parameters which can be fixed within uniaxial experimental tests. The parameters for the description of the concrete behaviour are: the energy release rate, the ultimate tensile strength, the compression strength and two fitting-parameters. The material model is implemented into a refined geometrically non-linear isoparametric hexahedral element with special formulations to reduce locking effects.

Keywords: Concrete behaviour, Multi-surface plasticity, Material modelling, Numerical simulation

1. Introduction

A realistic consideration of the structural behaviour of concrete constructions using the finite element method requires a three-dimensional description of the material and the element formulation. Three-dimensional finite elements are helpful to model the exact geometry of structures. Especially for boundaries, junction areas or similar this may be essential. To receive the realistic material behavior – like stresses and strains – a three-dimensional material model is indispensable. Many approaches for multiaxial models can be found in the literature which are based on the theory of plasticity but most of them are used with two-dimensional elements like plates or shells e.g. Hofstetter and Mang [1], Menrath [2] and many others. The model introduced here discusses the numerical description of pure, not reinforced concrete and is implemented in a hexahedral element.

2. Basic Ideas of the Numerical Model

2.1 The Composed Yield Functions

The introduced material law is based on a multi-surface plasticity theory for small strains. As all significant mechanisms of concrete occur within small strains, an additive split into elastic and inelastic parts

$$\mathbf{E} = \mathbf{E}^{el} + \mathbf{E}^{pl} \tag{1}$$

does not represent any restrictions. For the following formulation a division of the second Piola-Kirchhoff stress-tensor into a hydrostatic and a deviatoric part is necessary

$$\mathbf{S} = \mathbf{S}^H + \mathbf{S}^D \quad , \quad \mathbf{S}^D = [\mathbb{I} - \frac{1}{3}(\mathbf{1} \otimes \mathbf{1})]\,\mathbf{S} \quad . \tag{2}$$

The used material-law is a combination of three conical yield functions of the

Drucker-Prager-type, see Figure 1

$$f_j(\mathbf{S},\kappa_j) = |\mathbf{S}^D| + \alpha_j I_1(\mathbf{S}) - \sqrt{\frac{2}{3}}\, y_j(\kappa_j) = 0 \quad , \quad j = 1,2,3 \quad . \tag{3}$$

$\mathbf{S}^D$ denotes the deviatoric stress tensor, I_1 the first invariant of the stress tensor $\mathbf{S}$. α is a hardening-parameter, the yield stress y depends on the internal variable κ. The so called inverted cone f_3 is only used for numerical stability at hydrostatic tension. Furthermore a spherical surface with radius R and origin L for the compression area is part within the considered model

$$f(\mathbf{S},\kappa) = \sqrt{|\mathbf{S}^D|^2 + \frac{1}{9}(I_1 - L(\kappa))^2} - R(\kappa) = 0 \quad . \tag{4}$$

2.2 Parameters of the Model

It is possible to employ the results of well known uniaxial experimental tests for different concretes to choose the parameters of the yield functions for a realistic description of concrete behaviour. Using the tensile strength f_{ctm} and the energy release during cracking g_f the exponential softening, which occurs during tests in the tensile case, is formulated as

$$y_1(\kappa_1) = \beta_1\ f_{ctm}\ \exp\Big(-\frac{\kappa_1}{\kappa_1^u}\Big) \quad \text{with} \quad \kappa_1^u = \frac{g_f}{f_{ctm}} \quad . \tag{5}$$

The parameters α_1 and β_1 for the tension part of the yield surface are defined with the tensile strength f_{ctm} and the compressive strength f_{cm}

$$\alpha_1 = \sqrt{\frac{2}{3}}\frac{\gamma_1 f_{cm} - f_{ctm}}{\gamma_1 f_{cm} + f_{ctm}} \qquad , \qquad \beta_1 = \frac{2\gamma_1 f_{cm}}{\gamma_1 f_{cm} + f_{ctm}} \quad . \tag{6}$$

The fitting parameter γ_1 can be fixed by comparing with the two-dimensional tests of Kupfer or Ottosen which may be found e.g. in Hofstetter and Mang [1].

Considering uniaxial compression in experiments one observes that at around one third of the compressive strength square hardening begins. After the maximum strength square softening occurs. This behaviour is approximated by

$$y_2(\kappa_2) = \begin{cases} \beta_2 \, \frac{1}{3} f_{cm} \quad \left(1 + 4\dfrac{\kappa_2}{\kappa_e} + 2\left(\dfrac{\kappa_2}{\kappa_e}\right)^2\right) & , \quad \kappa_2 < \kappa_e \\ \beta_2 \, f_{cm} \quad \left(1 - \left(\dfrac{\kappa_2 - \kappa_e}{\kappa_2^u - \kappa_e}\right)^2\right) & , \quad \kappa_e \leq \kappa_2 < \kappa_2^u \quad . \end{cases} \tag{7}$$

With the energy release rate g_c it is possible to formulate

$$\kappa_e = \frac{4 f_{cm}}{3 E_{cm}} \qquad , \qquad \kappa_2^u = \frac{3 g_c}{2 f_{cm}} + \kappa_e \quad . \tag{8}$$

The values α_2 and β_2

$$\alpha_2 = \sqrt{\frac{2}{3}} \frac{\gamma_2 - 1}{2\gamma_2 - 1} \qquad , \qquad \beta_2 = \frac{\gamma_2}{2\gamma_2 - 1} \tag{9}$$

depend only on γ_2, which may be found in the same way as γ_1. The condition of a smooth transition between the sphere f_4 and the rest of the model defines the origin L and the radius R as

$$L(\kappa_2) = -\left(\sqrt{54}\,\alpha_2 + 2\right) \, \gamma_2 \, \sqrt{\frac{2}{3}} \, y_2(\kappa_2) \quad , \tag{10}$$

$$R(\kappa_2) = -\left(\sqrt{\frac{2}{3} + 6\,\alpha_2{}^2}\right) \, \gamma_2 \, \sqrt{\frac{2}{3}} \, y_2(\kappa_2) \quad . \tag{11}$$

2.3 Return-mapping algorithm

The numerical application is based on a local iteration to satisfy the principle of maximum dissipation with the yield-condition f as a constrain. Thus, an implicit Euler-backward algorithm is chosen to integrate the rate independent evolution equations for the inelastic strains and the internal variable.

An implicit time integration results in the classical return-mapping algorithm for the actual stress state, see Simo and Hughes [3]. Starting at the time n an elastic predictor leads to the so called trial stress state $\mathbf{S}^{tr}$. Than the plastic corrector is used to fulfil the Kuhn-Tucker-conditions at the end of the time step $n+1$ for all yield-functions

$$f_{j,n+1}(\mathbf{S}_{n+1}, \kappa_{n+1}) \leq 0 \quad , \quad \Delta\lambda_{j,n+1} \geq 0 \quad , \quad f_{j,n+1}\Delta\lambda_{j,n+1} = 0 \quad . \tag{12}$$

In Eq (12) the increment of the plastic parameter for time step n to $n+1$ is denoted by $\Delta\lambda_{n+1}$.

The reversed return mapping direction of the inverted cone leads to modified conditions

$$f_{j,n+1}(\mathbf{S}_{n+1}, \kappa_{n+1}) \geq 0 \quad , \quad \Delta\lambda_{j,n+1} \leq 0 \quad , \quad f_{j,n+1}\Delta\lambda_{j,n+1} = 0 \quad . \tag{13}$$

From all admitted yield surfaces (m) only a few number (z) will be activated for an arbitrary deformation state. To combine z active surfaces Koiter [5] gives a modified flow rule

$$\dot{\mathbf{E}}^{pl} = \sum_{i=1}^{z} \dot{\lambda}_i \, \partial_{\mathbf{S}} f_i \quad \text{with} \quad z \leq m \quad . \tag{14}$$

This has to be taken in account in the constitutive equation within the elastic-predictor and plastic-corrector procedure.

As an example a description of the return-mapping algorithm for one single conical surface is given. For the other cones and the sphere similar formulations occur.

At the first step of the algorithm an elastic increase of the strains is assumed

$$\mathbf{S}^{tr} = \mathbb{C}^{el} : (\mathbf{E}_{n+1} - \mathbf{E}_n^{pl}) \quad . \tag{15}$$

If the yield condition

$$f^{tr} = |\mathbf{S}^{D,tr}| + \alpha \; I_1(\mathbf{S}^{tr}) - k(\kappa_n) \quad \begin{cases} \leq 0 & : \text{ elastic state} \\ \geq 0 & : \text{ plastic state} \end{cases} \tag{16}$$

is violated, a local Newton iteration is used to get the incremental update of the plastic parameters $\Delta\lambda_{n+1}$ and κ_{n+1}. After updating stresses and strains

$$\mathbf{S}_{n+1} = \mathbf{S}^{tr} - \Delta\lambda_{n+1} \; \mathbb{C}^{el} : (\mathbf{n}_{n+1} + \alpha \; \mathbf{1}) \tag{17}$$

$$\mathbf{E}_{n+1}^{pl} = \Delta\lambda_{n+1} \; \partial_{\mathbf{S}} f_{n+1} \tag{18}$$

the elastoplastic tangent modulus for a conical part of the surface at the time-step n+1 can be formulated

$$\mathbb{C}_{n+1}^{ep} = \frac{d\mathbf{S}_{n+1}}{d\mathbf{E}_{n+1}} = \left[\mathbf{\Theta} \; - \frac{(\mathbf{\Theta} \; : \partial_{\mathbf{S}} f) \otimes (\mathbf{\Theta} \; : \partial_{\mathbf{S}} f)}{\partial_{\mathbf{S}} f : \mathbf{\Theta} \; : \partial_{\mathbf{S}} f - \partial_{\kappa} k} \right]_{n+1} \tag{19}$$

with the relations

$$\begin{aligned} \partial_{\mathbf{S}} f_{n+1} &= [\mathbf{n} + \alpha \; \mathbf{1}]_{n+1} \qquad & \partial^2_{\mathbf{SS}} f_{n+1} &= \left[\frac{1}{|\mathbf{S}^D|} \big([\mathbb{I} - \frac{1}{3}(\mathbf{1} \otimes \mathbf{1})] - \mathbf{n} \otimes \mathbf{n} \big) \right]_{n+1} \\ \mathbf{n} &= \frac{\mathbf{S}^D}{|\mathbf{S}^D|} & \mathbf{\Theta}_{\;n+1} &= \left[\mathbb{C}^{-1} + \Delta\lambda \; \partial^2_{\mathbf{SS}} f \right]_{n+1}^{-1} \qquad . \end{aligned} \tag{20}$$

At the end of each time-step the moduli of all of the z active parts of the yield-surface are coupled.

The Newton-Raphson method assures the quadratic convergence within the equilibrium iterations, see e.g. Simo and Hughes [3], Kahn and Huang [4].

2.4 Implementation

In contrast to many other works in which a three-dimensional model is implemented into a 2D finite element formulation, see e.g. Menrath [2] or Hofstetter and Mang [1], here a three-dimensional element is used. Therefore it is possible to take advantage of the 3D-description of the material for a realistic simulation in a multiaxial state. The model is implemented in a refined geometrically non-linear isoparametric hexahedral element with linear shape functions for the displacements. Assumed natural strains for shear stains and strains in the third direction as well as enhanced assumed strains are introduced to reduce locking effects. A detailed description of the element formulation can be found in Klinkel et al. [6].

3. Specification of the Yield Surface

The example of one cube-like element under simple loading is investigated to describe the correct behaviour of the numerical concrete model. The stresses acting in the first direction are set to the value of $S_{11} = \sigma$, while the axial stresses are set to the value of $S_{22} = S_{33} = F\,\sigma$ in which F is a factor. With these values the first invariant reads $I_1(F) = (1+2F)\ \sigma$ and the norm of the deviatoric part of the second Piola-Kirchhoff stresses $|\mathbf{S}^D(F)| = \sqrt{2/3}\ |1-F|\sigma$. Figure 2 shows the yield surface for the values $\gamma_1 = 3.0$, $\gamma_2 = 1.2$ and the ratio $f_{cm}/f_{ctm} = 10.0$, which approximate the material behaviour of concrete well. If a linear kinematic relation is assumed all loading paths will be linear with the constant gradient of the loading path

$\delta = |\mathbf{S}^D(F)|/I_1$. Five intersection points characterize the yield surface: P_1 and P_5 lie on the I_1-axis, while P_2, P_3 and P_4 are the intersections of the single yield surfaces f_1, f_2 and f_4. Additionally the sign of σ and the necessary value of F to reach the points are depicted in Table 1. The maximum stress before softening occurs is

$$\sigma_{max} = \sqrt{\frac{3}{2}} \frac{|\mathbf{S}^D|}{|1-F|} = \frac{\beta_i f_{ci}}{|1-F|} \left(\frac{1}{\frac{\delta}{\alpha_i} - 1} + 1 \right) \quad . \tag{21}$$

This relation is only valid for the conical surfaces f_i with $i = 1, 2$.

3.1 Tension Area

Within this area only surface f_2 is active, thus failure is characterized by exponential softening described in Eq (5). The area is limited by the points P_1, hydrostatic tension, and P_2, where the path reaches f_2 beforehand. Figure 3 shows stress-strain-curves for possible F. The hydrostatic tension state with $F = 1.0$ will activate the inverted cone f_3.

3.2 Mixed Area

The yield surfaces for tension f_1 and compression f_2 will both be activated within the mixed area. Firstly the square hardening mechanism of f_2 occurs, then exponential softening tension failure of f_1 steps in and determines the curve. The boundaries of this area lie between points P_2 and P_3.

3.3 Compression Area

To achieve failure in longitudinal direction the stresses σ get the opposite sign. The area between P_3 and P_4 is characterized by the yield cone f_2 whereas the area between P_4 and P_5 is described by the sphere. Since both areas follow the square hardening / softening law the stress-strain-curves will be similar and are shown together in Figure 3. The difference between the surfaces is obvious. In opposite to the sphere different loading cases limited by the cone have the same intersection point with the $\sigma = 0$ axis.

4. Conclusions

A three-dimensional model for concrete which is based on a multi-surface plasticity-theory for small strains has been introduced. The yield-surface is a combination of three conditions of Drucker-Prager type and one spherical part for the compression case. It is possible to get the necessary parameters for the three-dimensional formulation from uniaxial experimental tests. To take the advantage of the realistic description of the model it is implemented into a three-dimensional finite element formulation. An isoparametric geometrically non-linear hexahedral element with special interpolations of the shear-strains to reduce locking-effects is used. The numerical three-dimensional model reproduces the phenomenological behaviour of concrete in a multiaxial state very well.

References

[1] Hofstetter G and Mang HA. Computational Mechanics of Concrete Structures. Viehweg & Sohn, Braunschweig Wiesbaden, 1995.

[2] Menrath H. Numerische Simulation des nichtlinearen Tragverhaltens von Stahlverbundträgern. PhD thesis, Universität Stuttgart, Institut für Baustatik, 1999. Bericht-Nr. 29(1999).

[3] Simo JC and Hughes TJR. Computational Inelasticity, volume 7, Mechanics and Materials. Springer-Verlag, Interdisciplinary Applied Mathematics, New York, 1998.

[4] Kahn AS and Huang S. Continuum Theorie of Plasticity. John Wiley & Sons, Inc., New York, 1995.

[5] Koiter WT. Stress-strain relations, uniqueness and variational theorems for elastic-plastic materials with a singular yield surface. The Quarterly Journal of Mechanics and Applied Mathematics 1953; 11:350–354.

[6] Klinkel S, Gruttmann F and Wagner W. A continuum based three-dimensional shell element for laminated structures. Computers and Structures 1999; 71:43–62.

Figures and Tables

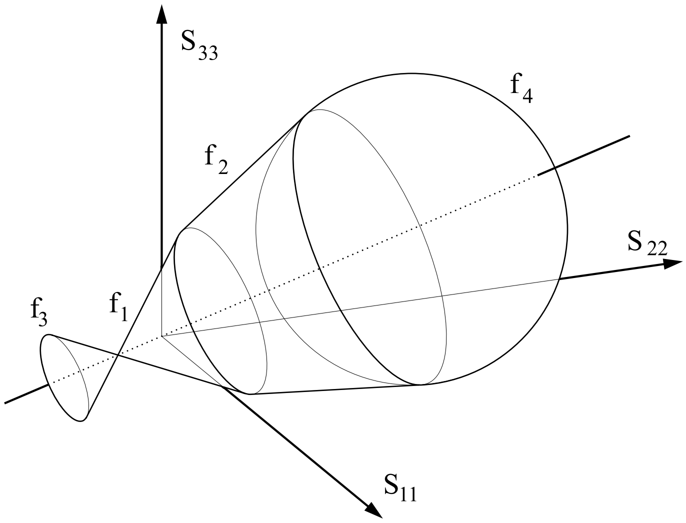

Figure 1: The combined yield surface

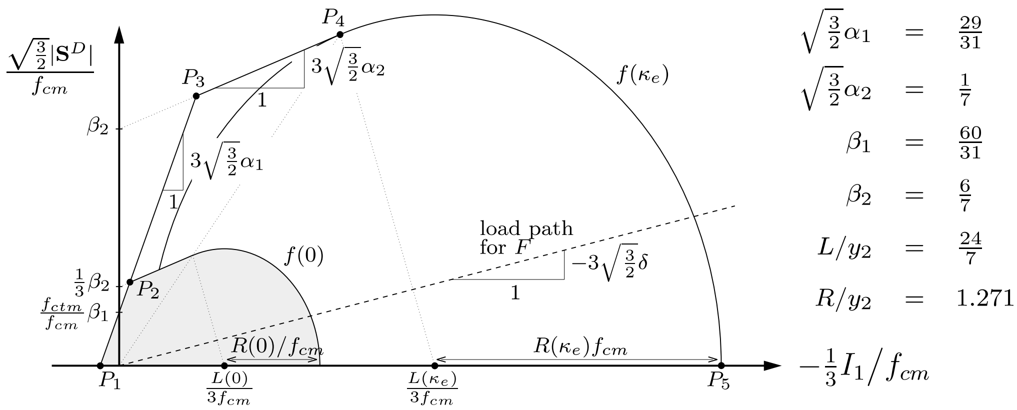

Figure 2: Exact geometry of the yield surface

Points	$\sqrt{\frac{3}{2}}\lvert\mathbf{S}^D\rvert$	I_1	$\sqrt{\frac{3}{2}}\delta$	σ	F	σ_{max}
P_1	0	$3\sigma_{max}$	0	$+$	1	$\frac{20}{29}f_{ctm}$
P_2	$\frac{13}{7}\lvert\sigma_{max}\rvert$	$-\frac{5}{7}\sigma_{max}$	$-\frac{13}{5}$	$+$	$-\frac{6}{7}$	$\frac{70}{43}f_{ctm}$
P_3	$\frac{21}{8}\lvert\sigma_{max}\rvert$	$-\frac{18}{8}\sigma_{max}$	$-\frac{7}{8}$	$+$	$-\frac{13}{8}$	$\frac{160}{43}f_{ctm}$
P_4	$\frac{3}{4}\lvert\sigma_{max}\rvert$	$-\frac{6}{4}\sigma_{max}$	$-\frac{1}{2}$	$-$	$-\frac{1}{4}$	$\frac{8}{5}f_{cm}$
P_5	0	$-3\sigma_{max}$	0	$-$	-1	$2.1809f_{cm}$

Table 1: Points on the yield surface

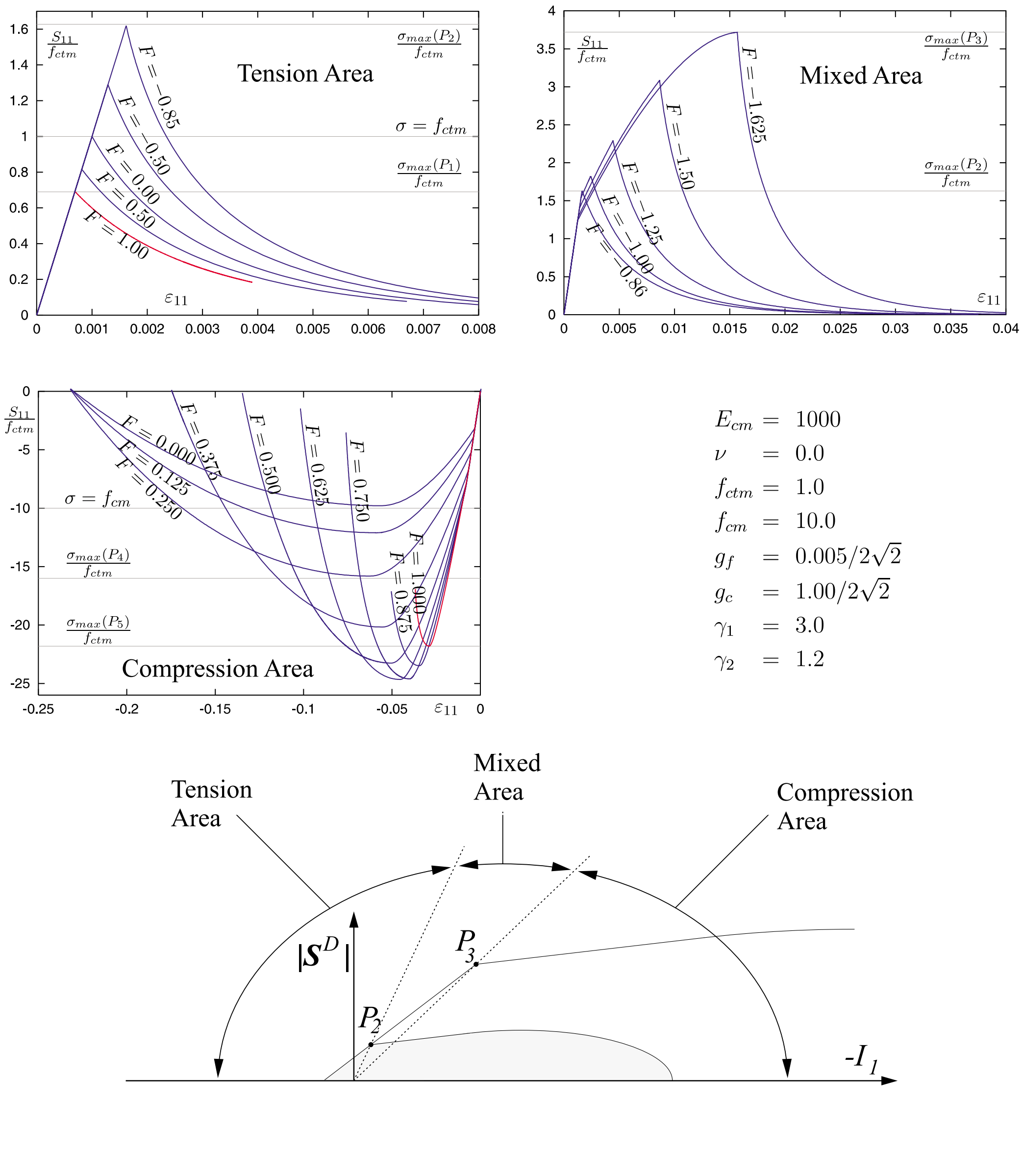

Figure 3: Different areas of the yield surface